Serbian Tribology Society

SERBIATRIB '19

16th International Conference on Tribology

Faculty of Engineering University of Kragujevac

Kragujevac, Serbia, 15 – 17 May 2019

DISTRIBUTION NON-UNIFORMITY OF THE ACCUMULATED PLASTIC STRAIN AT 3D SIMULATION OF SINGLE AND MULTI-ANGLED ECAE PROCESSES USING A MOVABLE RAM-DIE

Valentin KAMBUROV[1]*, Antonio NIKOLOV[1], Rayna DIMITROVA[1], Vladimir SEMENOV[2], Bogdan GILEV[1]

[1]Technical University of Sofia, Bulgaria

[2] Ufa State Aviation Technical University, Ufa, Russia

*Corresponding author: vvk@tu-sofia.bg

Abstract: Four virtual schemes for realizing the Equal Channel Angular Extrusion (ECAE) using a movable ram-die with different geometries of their deformation spaces (extrusion angles) have been developed and considered. On the basis of the performed simulations using CAD/CAM software, the data on the mean values of effective strain and their distribution are processed depending on the contact friction between the tool and the work-piece. The selected modes are compared and analyzed in terms of effective strain means and their dependence on contact friction. It has been found that the single-angled ECAE-MRD modes allow for a greater mean values of the effective strain compared to multi-angled ECAE patterns. It has been proven that the strain distribution non-uniformity and the filling of the deformation space depend on the contact friction.

Keywords: *severe plastic deformation, equal channel angular extrusion, CAD/CAE software 3D simulation, contact friction.*

1. INTRODUCTION

The Equal Channel Extrusion (ECAE) has been invented in the 1970's and it has been described first in [1]. The various SPD processes and regimes aim and result in the development of the ultra-fine grained (UFG) and nanocrystalline (NC) structure in the deformed under their recrystallization temperature materials [2, 3]. The most widely used scheme for severe plastic deformations (SPD) is ECAE based on simple shear, concentrated in a relatively narrow deformation section, between the intersecting grooves of the channels [4, 5]. As a processing operation, ECAE presents several significant technological advantages, the most important of which is the development of uniform, severe and localized steady simple shear in the transverse cross sections of deformed work-pieces [5, 6].

A major disadvantage to apply the ECAE deformation schemes, besides the limited length of the billets [7], is the contact friction force emerging between the work-pieces and the die channel walls, which increases the surface tension, strongly altering the distribution of stress-strain state in the volume of the deformed body [8]. A solution to this problem is proposed by providing some

movable parts of the deformation space - a moving ram-die and a fixed counter-support – ECAE-MRD [9, 10].

The present research introduces the results of a 3D simulation investigation, conducted to determine the distribution of the accumulated strains in an equal channel single and multi-angular extrusion with a movable ram-die and a counter-support as an effective technological scheme with limited friction forces. The deformation scheme and the tool equipment ensure a movable deformation space with two movable walls (ram-die) and a slightly mobile (related to two of the die-container walls) deformed work-piece.

The present research introduces the results of a 3D simulation investigation, conducted to determine the distribution of the accumulated strains in an equal channel single and multi-angular extrusion with a movable ram-die and a counter-support as an effective technological scheme with limited friction forces. The deformation scheme and the tool equipment ensure a movable deformation space with two movable walls of movable ram-die (ECAE-MRD) and a slightly mobile (related to two of the die-container walls) deformed work-piece.

2. MATERIALS AND METHODS

The three-dimensional modeling of the ECAE-MRD processes was performed at room temperature for a work-piece of deformable low-alloyed aluminum material having a cross-sectional dimension of 10.6 x 10.6 mm, a length of 70 mm (125 mm) and a ram-die movement speed of 5 mm/sec. The chosen lubricant is from package standard database with contact friction coefficient 0.05.

2.1 Virtual tool for Single-angled ECAE-MRD

The virtual tools to realize single-angled ECAE-MRD (Fig. 1) are composed from the following elements: die-container - 1; counter-support - 2; ram-die – 3; vertical channel - 4; - outlet calibration channel – 6. The vertical and calibration outlet channels are mutually intersecting (at an extrusion angle Φ), forming the zone of simple shear – 5 (Fig. 1). The virtual tools operate as follows: in the vertical channel 4 is placed the work-piece which, when moving the ram-die 2 downwards, is pushed (extruded) through the shear zone 5 in the outlet calibration channel 6. Extrusion is possible due to the counter-support 2 which closes the vertical channel 4. The processes of single angular extrusion with a movable ram-die and a rigid counter-support at different extrusion angles of channel crossing are simulated with the QForm VX 8.2.4 software (Fig. 1a and Fig. 1b).

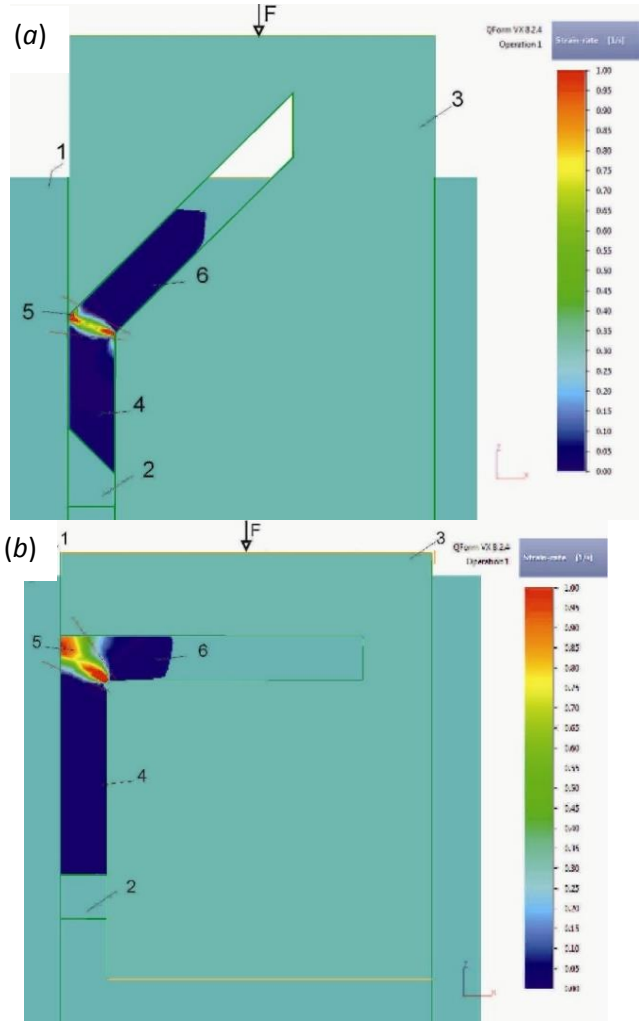

Figure 1. Virtual tool (QForm VX 8.2.4) for realizing single-angled ECAE-MRD, with strain rate distribution: (a) at an extrusion angle Φ=135^{O}; (b) at an extrusion angle Φ=90^{O}

Figure 1 shows the strain rate distribution in the scheme for realization of a single angular ECAE-MRD with an extrusion angle of intersection of the two channels: (a) Φ=135^{O} and (b) Φ=90^{O}.

2.2 Virtual tools for Multi-angled ECAE-MRD

The ECAE pattern with a movable ram-die can also be used to realize a multi-angular extrusion at intersection angles of 135^{O} for the channels. The processes of two-angled and four-angular equal channel extrusion with a movable ram-die were simulated with the QForm VX software (Figs. 2 and 3).

The virtual tool to realize a two-angled ECAE-MRD (Fig. 2) is composed of the following elements: die-container - 1; counter-support - 2; movable ram-die - 3. The deformation space is located in the ram-die and it consists of: a vertical channel - 4 (in which the work-piece is placed); and two crossed at an extrusion angle of 135^{O} channels - 6 and 7. The virtual tool for the two-angled ECAE operates as follows: a work-piece is placed in the vertical channel 4, moves through SPD zone 5 in the channel 7 after movement of the ram-die 3 downward, cross the deformation SPD zone 5A and enters the calibration channel 6 (Fig. 2 (a)).

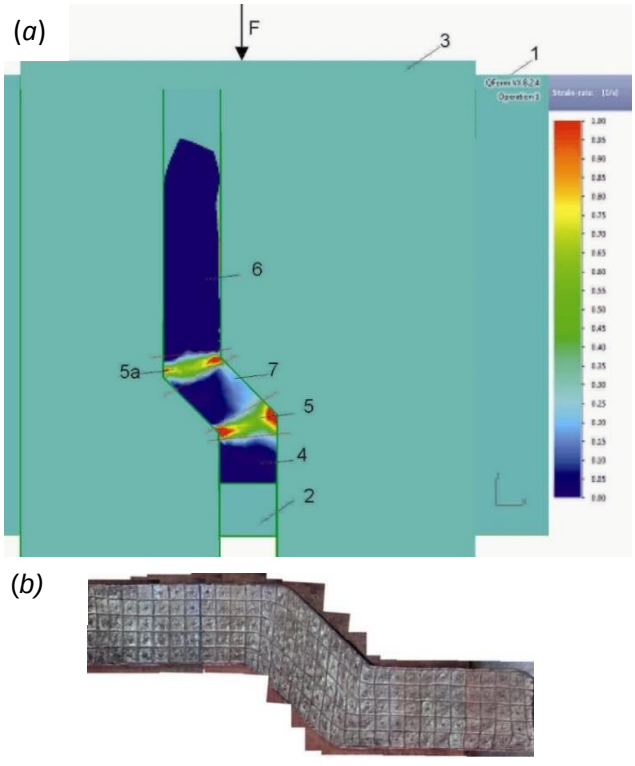

Figure 2. Two-angled ECAE-MRD at an extrusion angle Φ=135^{O}: (a) strain rate distribution (QForm VX 8.2.4); (b) deformed lead work-piece with a plotted coordinate grid

The virtual tool to realize a four-angled ECAE-MRD (Fig. 3) consists of the following elements: die-container - 1; counter-support - 2; movable ram-die - 3. The deformation space is located in the ram-die 3 and it consists of a vertical channel 4 (in which the metal work-piece is placed) and of crossed at an extrusion angle of 135^{O} channels - 7, 8, 9 and 6.

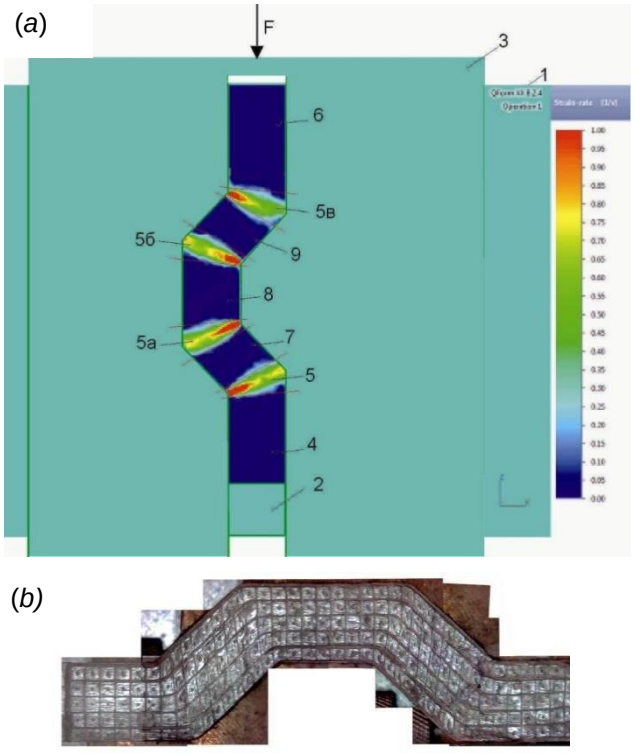

Figure 3. Four-angled ECAE-MRD at an extrusion angle Φ=135^{O}: (a) strain rate distribution (QForm VX 8.2.4); (b) deformed lead work-piece with a plotted coordinate grid

The virtual tool for a two-angled ECAE-MRD operates as follows: in the vertical channel 4 is placed the work-piece which, when moving the ram-die 3, is pushed out (extruded) and passes successively through the shear zone 5, the channel 7, the second shear zone 5a, the parallel channel 8, the third shear zone – 5b, the inclined channel - 9, the fourth deformation zone – 5c and finally entering the calibration channel - 6 (Fig. 2b)).

2.3 Determination of the Average Values of the Effective Strain

The magnitude of the equivalent effective plastic strain in single ECAE in a frictionless

mode it was accepted to be determined according to the dependence [15]:

$$\varepsilon_{eff} = \frac{N}{\sqrt{3}}\left[2\cot\left(\frac{\Phi+\Psi}{2}\right)+\frac{\psi}{\sin\left(\frac{\Phi+\Psi}{2}\right)}\right] \quad (1)$$

where: ε_{eff} – the effective plastic strain, Φ is the extrusion angle between the two intersecting channels; Ψ is the die channel angle determined by the inner radius of curvature; N – the number of passes.

The mean values of the effective plastic strain obtained by a computer simulation (QForm VX 8.2.4) of the shown in Fig. 1, Fig. 2 and Fig. 3 schemes for single and multi-angled ECAE in the frictionless mode are given in Table 1. The values of the effective strain determined by formula (1) at Ψ=0 are given in brackets.

Table 1. Sample mean results of effective plastic strain from simulation of one-angled and multi-angled ECAE-MRD under frictionless conditions

Pass number x die channel angle	Effective plastic strain values - sample means of computer simulations under frictionless conditions (2) and - according to the formula (1) in brackets			
	One-angled x135°	**One-angled x90°**	**Two-angled x135°**	**Four-angled x135°**
First pass 1x135°	0.49 (0.48)	-	0.58 (0.48)	0.58 (0.48)
Pass 2x135° or 1x90°	0.97 (0.96)	1.00 (1.16)	1.00 (0.96)	1.01 (0.96)
Third pass 3x135°	1.48 (1.44)	-	1.44 (1.44)	1.54 (1.44)
Pass 4x135° or 2x90°	1.99 (1.92)	2.12 (2.31)	1.98 (1.92)	1.99 (1.92)

The close values for the effective strain obtained by calculation by the expression (1) and the computer simulation (Table 1) confirmed the claim that the deduced formula (1) does not take into account the contact friction and consequently the strain distribution uniformity [16].

The determination of the distribution of the plastic strain in the volume of the deformed work-piece is related not only to the averaging of the so-called sample mean, but also by determining their standard deviation values. In the numerical determination of the strain distribution non-uniformity it is accepted to use the standard deviation S_D or simply s:

$$S_d = s = \sqrt{\frac{1}{n-1}\sum_{n-1}^{n}(\varepsilon_i - \bar{\varepsilon})^2} \quad (2)$$

where: n - the number of nodes in the cross-section (in this case n = 49); ε_i - the magnitude of effective plastic strain at certain nodes of the deformed body; $\bar{\varepsilon}$ - the sample mean of the plastic strain at all nodes of the selected cross section of the deformed body

$$\bar{\varepsilon} = \frac{1}{n}\sum_{i=1}^{n}\varepsilon_i \, . \quad (3)$$

The hypothesis will be examined whether the sampling averages of the effective strain for different ECAE-MRD (from the rows of Table 1) are equal [17]. For convenience, the two effective deformations obtained for different strain modes (Table 1) are denoted with X and Y , i.e. $X = \varepsilon$ for a deformation scheme (from Table 1), and $Y = \varepsilon$ for another deformation scheme (from Table 1). Then the difference between the two sample means is also normally distributed, i.e.:

$$Z_{\bar{X}-\bar{Y}} = \frac{(\bar{X}-\bar{Y})-(\mu_x-\mu_y)}{\sqrt{\frac{s_x^2}{n_x}+\frac{s_y^2}{n_y}}} \in N(0,1) \, . \quad (4)$$

where: n_x n_y are the numbers of observations of the effective strains in those deformation modes - $n_X = n_Y$=49>30. If $Z_{\bar{X}-\bar{Y}} \in$[-2.56, 2.56] it can be accepted with a confidence level) $\alpha = 0.01$ the basic hypothesis, i.e. that those the two sample means $\bar{X}$ and $\bar{Y}$ are equal.

3. SIMULATIONS AND RESULTS

3.1 Distribution of the Effective Strain in Single-angled ECAE-MRD at 135^O

In the computer simulation of a one-angled ECAE with a movable ram-die at an extrusion

angle of 135° with contact friction, it was found that the deformed work-piece completely fills the deformation space. The effect of contact friction in the one angular (135^O) ECAE-MRD mode is also expressed in increasing the effective strain at the four corners of the deformed work-piece, with the middle section of the transverse cross-section being less deformed (Fig. 4).

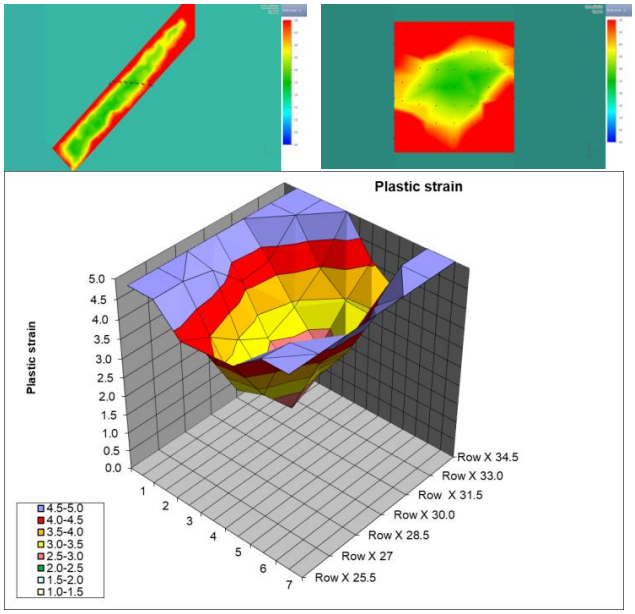

Figure 4. Effective plastic strain distribution (QForm VX 8.2.4) within the deformed by one-angled ECAE-MRD work-piece (at an extrusion angle Φ=135^O) after fourth pass (4x135^O)

The sample mean values of the effective strain after a second pass (2x135^O) is ε_{eff}=2.37 (varies between ε_{min}=1.16 in the middle and ε_{max}=3.96), with a standard deviation of 1.43. After four passes (4x135^O), a similar distribution and an effect of the contact friction is recorded (Fig. 4). The sample mean values of the effective strain after the fourth pass increases and is ε_{eff}=5.22 (ranges between ε_{min}=3.15 in the middle and ε_{max}=9.14), and the standard deviation increases to 2.08.

3.2 Distribution of the Effective Strain in Single-angled ECAE-MRD at 90^O

In the computer simulation of a one-angled ECAE with a movable ram-die at an extrusion angle of 90° with contact friction, it was found that the deformed work-piece filled the deformation space completely. The effect of the contact friction in the one-angled (90^O) ECAE-MRD diagram is also expressed in the increase of the effective strains from the outer wall of the deformed work-piece, the rest of the cross-section being less deformed. After the second pass (2x90^O), a similar effect of contact friction and symmetrical distribution on both sides is observed (Fig. 5).

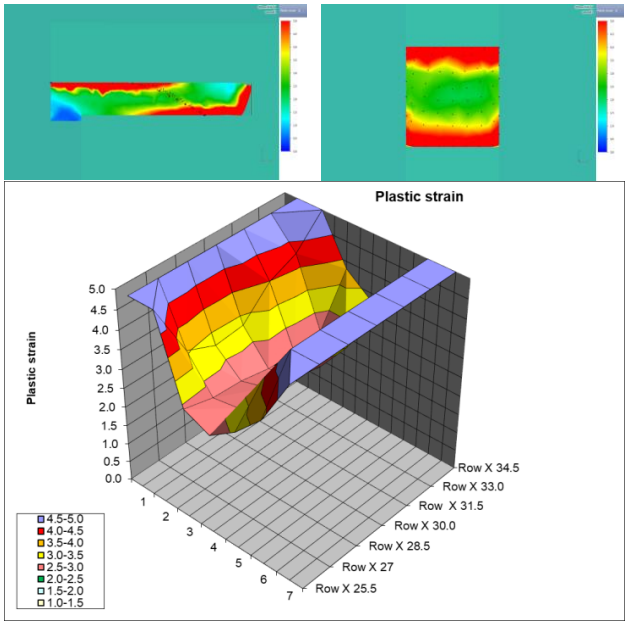

Figure 5. Effective plastic strain distribution (QForm VX 8.2.4) within the deformed by one-angled ECAE-MRD work-piece (at an extrusion angle Φ=90^O) after second pass (2x90^O)

The sample mean values of the effective strains after a second pass (1x90^O) is ε_{eff}=2.21 (ranges between ε_{min}=1.06 and ε_{max}=7.26), with a standard deviation of 1.92. The sample mean values of the effective strains after a second pass (Fig. 5) increases and is ε_{eff}=4.87 (varies between ε_{min}=2.69 and ε_{max}=8.40) and the standard deviation increases insignificantly to 2.11.

3.3 Distribution of the Effective Strain in Two-angled ECAE-MRD at 135^O

From the representation of the effective strain in a computer simulation of a two-angled ECAE-MRD with contact friction reading at 2x135^O angles after a first transition (2x135^O) it is evident that they are unilaterally concentrated on one side of the deformed work-piece and after a second pass (4x135^O) – on both sides (Fig. 6).

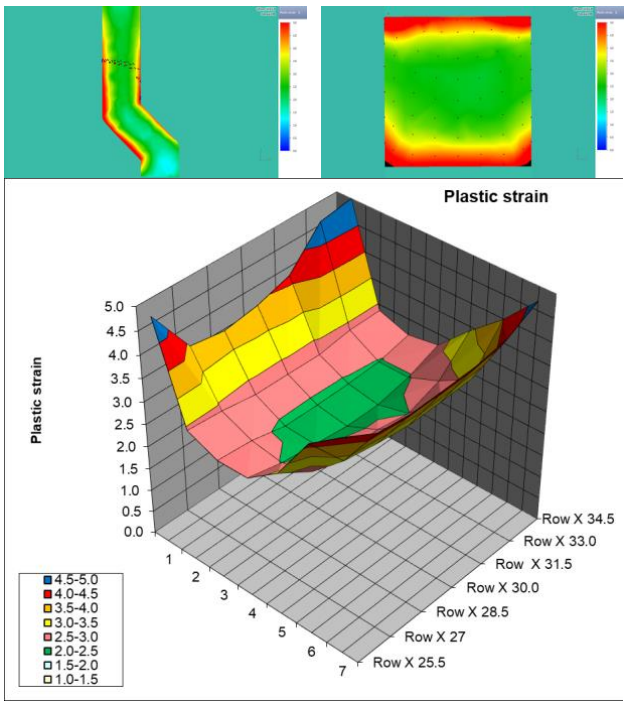

Figure 6. Effective plastic strain distribution (QForm VX 8.2.4) within the deformed by two-angled ECAE-MRD work-piece (at two extrusion angles Φ=135^{O}) after second pass (4x135^{O})

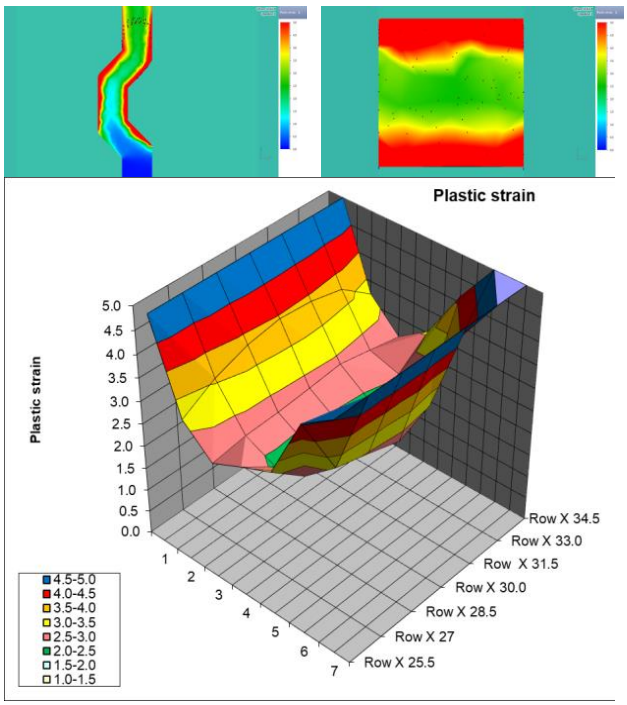

Figure 7. Effective plastic strain distribution (QForm VX 8.2.4) within the deformed by four-angled ECAE-MRD work-piece (at four extrusion angles Φ=135^{O}) after single pass (4x135^{O})

The sample mean values of the effective strain after a second pass is ε_{eff}=1.66 (varies between ε_{min}=1.16 and ε_{max}=3.40), with a standard deviation being relatively low 0.79. The sample mean values of the effective strain after the fourth pass (Fig. 6) increases and is ε_{eff}=3.27 (varies between ε_{min}=2.47 and ε_{max}=4.61) and the strain distribution (the standard deviation) remains relatively low – 0.85.

3.4 Distribution of the Effective Strain in Four-angled ECAE-MRD at 135^{O}

From the representation of the effective strain in a computer simulation of a four-angle ECAE-MRD with a contact friction reading at 4x135^{O} angles, after crossing of the two (firs and second) shear zones (2x135^{O}) shows that they are bilaterally concentrated, but it remains on both sides after crossing the remainder two (third and fourth) zones (4x135^{O}) (Fig. 7).

The sample mean values of the effective strain after the first two zones is ε_{eff}=2.52 (ranges between ε_{min}=1.37 and ε_{max}=4.72), with a standard deviation of 1.22.

The sample mean values of the effective strain after crossing and the fourth zone (Fig. 7) increases to ε_{eff}=3.80 (ranges between ε_{min}=2.45 and ε_{max}=5.68) and the strain distribution (the standard deviation) is 1.36.

4. DISCUSSION

The results of the sample mean values of the effective strain, taking into account the contact friction shown in the modes of Fig. 1, Fig. 2 and Fig. 3 for single- and multi-angular ECAE-MRD with a contact friction reading are given in Table 2. Highest values of the accumulated effective strain at the same deformation angles were obtained with single-angled ECAE-MRD (90° and 135°) and the lowest were obtained for the two-angled ECAE-MRD (135°).

The determined effective strains in the selected deformation modes under contact friction conditions are 1.6 to 2.5 times higher than those obtained in the frictionless conditions (Table 1). The increase in the sample mean values of the effective strain by ECAE-MRD as well as the overall filling of the deformation space is due entirely to the

contact friction between the deformed work-piece and the tool walls.

Table 2. Sample mean results $\overline{X}$ of effective strain from simulation of one-angled and multi-angled ECAE-MRD taking into account contact friction

Pass number x die channel angle	Effective plastic strain (sample means) taking into account friction			
	One-angled x135°	**One-angled x90°**	**Two-angled x135°**	**Four-angled x135°**
First pass 1x135°	0.96	-	1.05	1.25
Pass 2x135° or 1x90°	2.37	2.21	1.66	2.52
Third pass 3x135°	3.71	-	3.01	3.47
Pass 4x135° or 2x90°	5.22	4.87	3.27	3.80

The results of the determined strain distribution (the standard deviation) in the transverse cross section of the deformed bodies are given in Table 3. The highest non-uniformity of the effective strain is characterized by the single-angled ECAE-MRD mode at 90^{O} (Fig. 5) and the smallest – the two-angled ECAE-MRD (Fig. 6).

Table 3. Strain distribution uniformity of computer simulations taking into account friction expressed through standard deviation values $\mathbf{S_D}$

Pass number x die channel angle	Effective plastic strain (sample means) taking into account friction			
	One-angled x135°	**One-angled x90°**	**Two-angled x135°**	**Four-angled x135°**
First pass 1x135°	0.82	-	0.60	0.66
Pass 2x135° or 1x90°	1.43	1.92	0.79	1.22
Third pass 3x135°	1.76	-	1.17	1.40
Pass 4x135° or 2x90°	1.76	2.11	0.85	1.36

The increase in the standard deviation, i.e., the non-uniformity of the strains as a result of the contact friction reading varies with the various ECAE-MRD modes.

The observed value of $Z_{\overline{X}-\overline{Y}}$ (Tables 4–7), by which we judge whether to accept the basic hypothesis of equality of sampling averages, i.e. if $Z_{\overline{X}-\overline{Y}}$ is within the confidence interval [-2.56, 2.56], then the sample means are assumed to be equal. Otherwise it is assumed that they are not equal.

Table 4. Normalized difference $Z_{\overline{X}-\overline{Y}}$ of sample means $\overline{X}$ and $\overline{Y}$ from the first pass $1x135^{O}$

First pass 1x135°	Two-angled 1x135°	Four-angled 1x135°
One-angled 1x135°	-0.86	-2.18
Two-angled 1x135°	-	-1.58

The comparisons of the sample means $\overline{X}$ of the first row of Table 2 (first transition 1x135°) are given in Table 4. They can be considered equal, because their $Z_{\overline{X}-\overline{Y}}$ are within the range [-2.56, 2.56].

Table 5. Normalized difference $Z_{\overline{X}-\overline{Y}}$ of sample means $\overline{X}$ and $\overline{Y}$ from the pass $2x135^{O}$ or $1x90^{O}$

Pass 2x135° or 1x90°	One-angled 1x90°	Two-angled 2x135°	Four-angled 2x135°
One-angled 2x135°	0.44	3.04	-0.57
One-angled 1x90°	-	2.27	-1.60
Two-angled 2x135°	-	-	-4.15

Table 6. Results of normalized difference $Z_{\overline{X}-\overline{Y}}$ of sample means $\overline{X}$ and $\overline{Y}$ from the pass $3x135^{O}$

Third pass 3x135°	Two-angled 3x135°	Four-angled 3x135°
One-angled 3x135°	2.33	0.75
Two-angled 3x135°		-1.76

The comparisons of the second row of Table 2 (transition 2x135° or 1x90 °) are given in Table 5. They can be assumed to be equal

(except for $\overline{X}$ =1.66), because their respective values $Z_{\overline{X}-\overline{Y}}$ are outside the range.

The comparisons from the sample averages $\overline{X}$ from the third row of Table 2 (transition 4x135° or 2x90°) are given in Table 5. They can be assumed to be equal because their $Z_{\overline{X}-\overline{Y}}$ are within the range [-2.56, 2.56].

Table 7. Normalized difference $Z_{\overline{X}-\overline{Y}}$ of sample means $\overline{X}$ and $\overline{Y}$ from the pass 4x135^{O} or 2x90^{O}

Pass 4x135° or 2x90°	One-angled 2x90°	Two-angled 4x135°	Four-angled 4x135°
One-angled 4x135°	0.83	6.07	3.99
One-angled 2x90°		4.91	2.97
Two-angled 4x135°			-2.33

The comparisons from the sample averages $\overline{X}$ of the fourth row of Table 2 (transition 4x135° or 2x90°) indicate that the first two (single-angled) and second two (multi-angled) can be considered equal.

5. CONCLUSIONS

1. It has been found that the single-angled ECAE-MRD modes allows for a greater mean values of the effective strain compared to multi-angled ECAE-MRD patterns at the same (resultant) value of their extrusion angles.
2. Using computer simulations, it is confirmed that the used dependence (1) for determining the effective strain does not take into account the contact friction and consequently caused by it the non-uniformity of the effective strain.
3. The determined values of ECAE-MRD accumulated effective strains with contact friction are 1.6 to 2.5 times higher than the values obtained in the simulation of the processes under the frictionless conditions.
4. It was found that contact friction rather than the type of the strain space of the ECAE modes under consideration is the main cause of the non-uniform distribution of effective strains, with the highest non-uniformity of the strains being considered in the single-angled ECAE-MRD mode at 90°, smaller – at the two-angled ECAE-MRD mode at 135°.
5. In the test for the equality of sample averages of effective strain (taking into account the contact friction) it was found that although the extrusion angles of the intersecting grooves in the ECAE are equal, it is not always the mean values of the effective strain that can be assumed to be equal.

ACKNOWLEDGEMENT

The authors thank the eng. N. Radeva and eng. A. Yordanov, who helped to perform the computer simulation with the specialized software product Quantor Form VX 8.2.4. The authors would like to thank the Research and Development Sector at the Technical University of Sofia for the financial support.

REFERENCES

[1] V.M. Segal: *The Method of Material Preparation for Subsequent Working,* Invention Certificate of the USSR No. 575892, 1977.

[2] V.M. Segal: *Equal channel angular extrusion: from macromechanics to structure formation*, Materials Science and Engineering 1999, A 271 (1-2): 322–333.

[3] G.J. Raab, R.Z. Valiev, T.C. Lowe, Y.T. Zhu: *Continuous processing of ultrafine grained Al by ECAP-Conform*, Materials Science and Engineering 2004, A 382, 30–34.

[4] R.Z. Valiev, T.G. Langdon: *Principles of equal-channel angular pressing as a processing tool for grain refinement*, Progress in materials science 51, 2006, 881-981.

[5] V.M. Segal, V.I. Reznikov, A.E. Drobyshevski, V.I. Kopylov: *Plastic working of metals by simple shear*, Russ. Metall. (Engl. Transl.) 1981, vol. 1, 99–105.

[6] J.G. Genov: *Energetic Interpretation of Limit Steady Forming of Sheet Metal*, Journal of Material Science and Technology (14, 2) 2006, ISSN 0861-9786, 75–86.

[7] V.M. Segal: *Engineering and commercialization of equal channel angular extrusion (ECAE)*, Materials Science and Engineering A 386 2004, 269–276.
[8] M. Kandeva: *The Contact Approach in Engineering Tribology*, Publishing House Technical University – Sofia, Sofia, 2012, 505 p. (in Bulgarian).
[9] A.A. Nikolov: *Construction schemes for severe plastic deformation of metals using equal channel angular extrusion*, PhD Thesis, Technical University of Sofia 2016, Sofia (in Bulgarian).
[10] V.V. Kamburov, V.I. Semenov, N.T. Tontchev, V.P. Mishev, A.A. Nikolov: *3D simulation by CAD/CAE software of the deformation process at equal channel angular extrusion with active friction forces*, XIV Int. Congress "Machines, Technologies, Materials 2017" Varna, 2017, Proceedings year I, Issue 6(6) vol. VI, 423-426.
[11] S. Letzkovska, P. Rahnev, J. Genov, K. Semenliyski: *Computer based equipment for measuring of limited deformation*, XXXVII Int. conf. on Information, Communication and Energy systems and Technologies, Niš 2002, Yugoslavia Proceedings of papers, vol.1, 168-169.
[12] K. Kamberov, G. Todorov, Sv. Stoev, B. Romanov: *Mechanical Strenght Test of Train Wheel Based on Virtual Prototyping*, Proceedings in Manufacturing Systems, 2015, vol. 10, issue 3, 99 – 104.
[13] N. Tontchev: Materials Science, Effective solutions and Technological variants, LAMBERT Academic Publishing, (2014) 142 p.
[14] N. Tontchev, Z. Cekerevac: *Approach and Application in Multicriteria Decision Support in the Field of Materials Science*, MEST Journal, (MEST, 2014, no. 118-29.
[15] Y. Iwahashi, J. Wang, Z. Horita, M. Nemoto, T. Langdon: *Principle of Equal-Channel Angular Pressing for the Processing Of Ultra-Fine Grained Materials*, Scr. Mater., 1996, 35, 143–146.
[16] F. Djavananroodi, B. Omranpour, M. Ebrahimi, M. Sedigli: *Designing of ECAP parameters based on strain distribution uniformity*, Chinese Materials Research Society, Progress in Natural Science: Materials International 2012, 22(5), 452-460, http://doi.org/10.1016/j.pnsc.2012.08.001.
[17] J.E. Freund: *Mathematical Statistics with Applications (eighth edition)*, Pearson Education Limited, 2014, ISBN 10: 1-292-02500-X.